Buoyancy-driven motion of bubbles and droplets in EVP fluids

Giancarlo Esposito, Yannis Dimakopoulos, John Tsamopoulos [1]

Scientific collaboration – O. Tammisola, K. Tassawar, A. Balasubramanian [2]

Basilisk Users' Meeting 2023
Paris
07-07-2023

This project received funding from the European Union's Horizon 2020 research and innovation program under the Marie Skłodowska-Curie grant agreement No 955605

(1) The FLUIDS LAB – Laboratory of Fluid Mechanics and Rheology

(2) KTH FLOW

University of Patras – Department of Chemical Engineering – ChemEngUP

ΠΑΝΕΠΙΣΤΗΜΙΟ ΠΑΤΡΩΝ – UNIVERSITY OF PATRAS

YIELDGAP – YIELD-stress fluids beyond Bingham

SORBONNE UNIVERSITÉ

Elasto-visco-plasticity

Rearrangement of the macromolecules and memory effects

Dissipative effects, resistance to flow, irreversibility

Solid behaviour up to a certain level of applied stress (yield-stress)

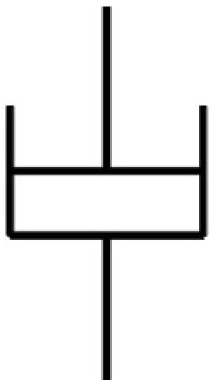

Examples of yield stress materials

- **Paints**
- **Mayonnaise (Emulsions)**
- **Concrete**
- **Toothpaste**
- **Gels**

Mechanisms:

Jammed (repulsive)

Networked (attractive)




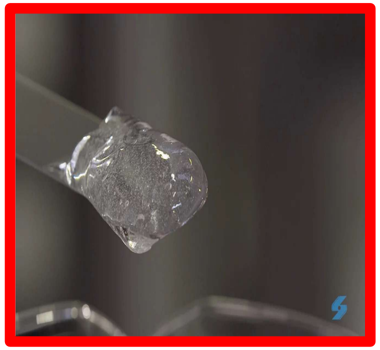
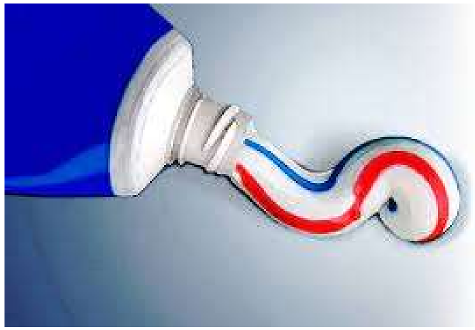


How the presence of bubbles and droplets affects the properties of these materials?

Desired	Unwanted
• Aerated Chocolate • Cosmetic products • Toothpaste • Sewage sludge	• Cement failures • Oil extraction

Evolution of models

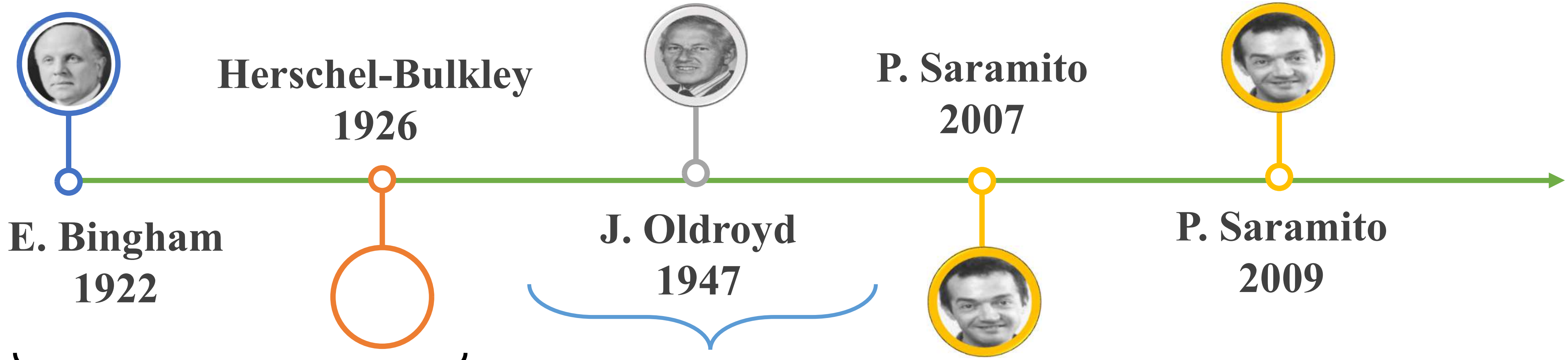

Scalar viscoplastic (rigid solid
+
Generalized Newtonian fluid)

$$\tau = \begin{cases} 0 & \tau \le \tau_y \\ \tau_y + \eta_p \dot{\gamma} & \tau > \tau_y \end{cases}$$

Tensorial viscoplastic
(elastic solid
+
Generalized Newtonian
fluid)

$$\tilde{\boldsymbol{\tau}} = \begin{cases} G\tilde{\boldsymbol{\gamma}} & |\tilde{\tau}| < \tau_y \\ \left(\eta_p + \frac{\tau_y}{|\dot{\gamma}|}\right)\tilde{\dot{\boldsymbol{\gamma}}} & |\tilde{\tau}| \ge \tau_y \end{cases}$$

Elastoviscoplastic
model

$$\frac{1}{G}\overset{\nabla}{\tilde{\boldsymbol{\tau}}} + \max\left(0, \frac{|\boldsymbol{\tau}| - \tau_y}{k|\boldsymbol{\tau}|^n}\right)^{\frac{1}{n}} \tilde{\boldsymbol{\tau}} = \tilde{\dot{\boldsymbol{\gamma}}}$$

Do Yield Stress materials exhibit elasticity?

Negative wake

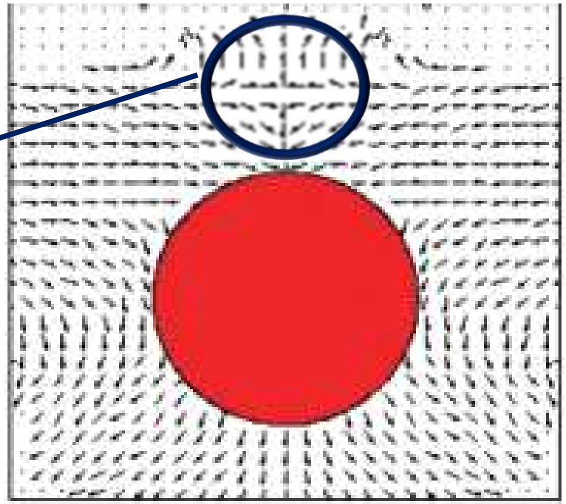

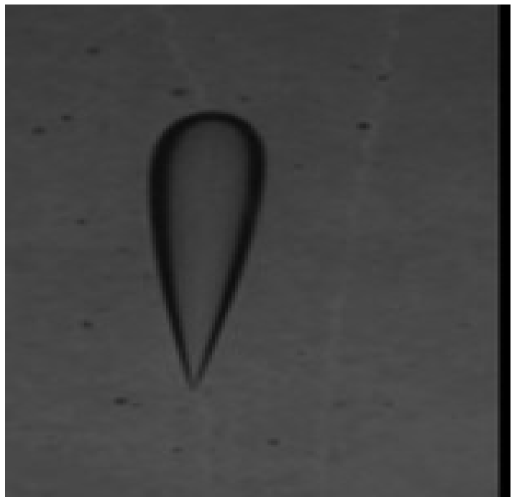

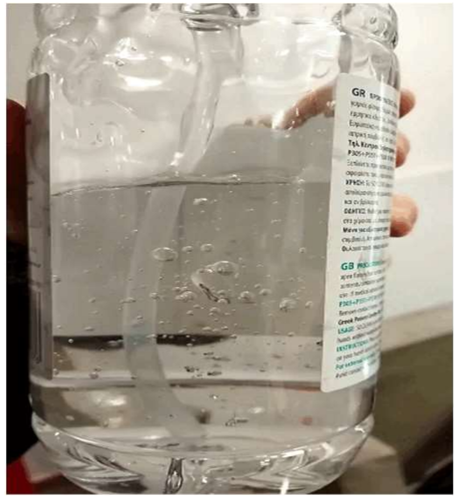

Holenberg et al., PRE, 2012, **Negative wake** behind a sphere sedimenting in Carbopol.
Rupture of the fore-aft-symmetry in creeping flow

Lopez et al., 2018, air bubble rising in Carbopol. This inverted teardrop shape is characteristic of bubbles rising in VISCOELASTIC materials

Giancarlo Esposito, while waiting for a delicious pita gyros in Patras

Problem formulation

$\nabla \cdot \boldsymbol{u} = \boldsymbol{0}$ ***Continuity equation (Mass balance)***

$\frac{\partial \boldsymbol{u}}{\partial t} + \boldsymbol{u} \cdot \boldsymbol{\nabla u} = -\frac{1}{\rho}[\boldsymbol{\nabla}\mathrm{P} + \nabla \cdot \bar{T}] - g\boldsymbol{e_z} + \boldsymbol{f_\sigma}$ ***Momentum balance***

$\bar{T} = \eta_s(\overline{\boldsymbol{\nabla u}} + \overline{\boldsymbol{\nabla u}^T}) + \bar{\boldsymbol{\tau}}$ ***Deviatoric total stress tensor***

$\frac{1}{G}\overset{\nabla}{\bar{\boldsymbol{\tau}}} + \max\left(0, \frac{\tau_d - \tau_y}{k\tau_d^n}\right)^{\frac{1}{n}} \bar{\boldsymbol{\tau}} = \overline{\boldsymbol{\nabla u}} + \overline{\boldsymbol{\nabla u}^T}$ ***Rheological constitutive equation (SHB)***

Kelvin-Voigt viscoelastic solid

Shear thinning Viscoelastic liquid

$$\tau_d = \left(\frac{1}{2}\bar{\boldsymbol{\tau}}:\bar{\boldsymbol{\tau}}\right)^{\mathbf{0.5}}$$

Von Mises criterion $\boldsymbol{\tau_d > \tau_y}$

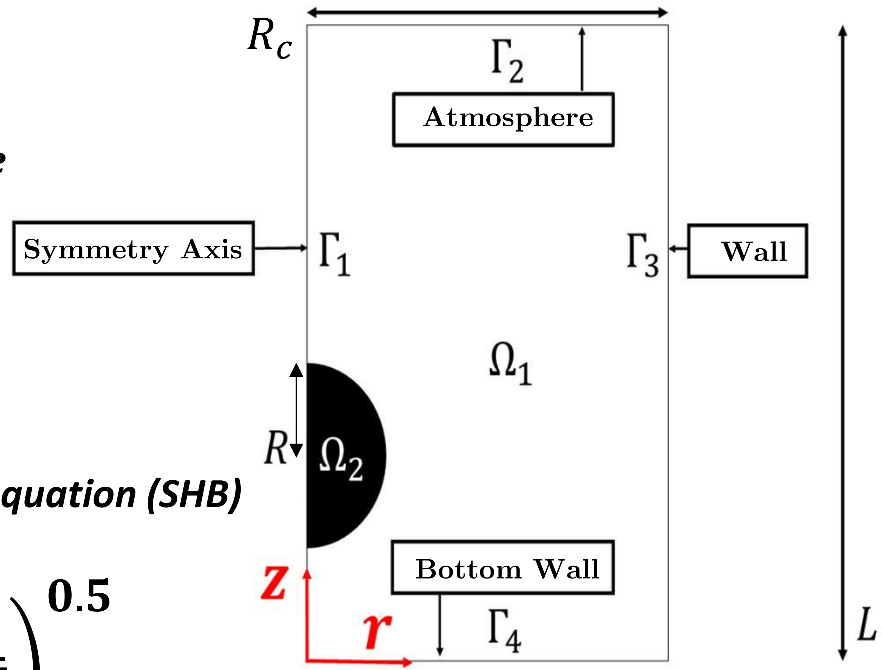

$L = 40R$
$R = 20R$

Numerical approach

- The numerical simulations are carried out with **Basilisk.**
- **Single fluid-formulation,** the physical properties are weighted averages of the physical properties of each phase.
- The **V.O.F method** is employed for the interface-capturing.
- The **log-conform.h** is modified to implement the Saramito-Herschel-Bulkley constitutive equation.

$$\rho(\phi) = \rho_1\phi + \rho_2(1-\phi), \qquad \eta(\phi) = \frac{1}{\frac{1}{\eta_1}\phi + \frac{1}{\eta_2}(1-\phi)}$$

Numerical approach

$$\bar{\nabla} = \frac{1}{R}, \, [\bar{\tau}, \bar{P}] = \rho_1 g R, \bar{U} = \sqrt{gR}$$

- $\nabla \cdot \tilde{\boldsymbol{u}} = \mathbf{0}$
- $\frac{\partial \tilde{\boldsymbol{u}}}{\partial \tilde{t}} + \tilde{\boldsymbol{u}} \cdot \tilde{\nabla} \tilde{\boldsymbol{u}} = \frac{1}{\tilde{\rho}} \left[-\tilde{\boldsymbol{\nabla}} \tilde{P} + \frac{\beta}{Ar} \tilde{\nabla}^2 \tilde{\boldsymbol{u}} + \frac{1}{Bo} \widetilde{\boldsymbol{f}_{\boldsymbol{\sigma}}} + \tilde{\boldsymbol{\nabla}} \cdot \tilde{\boldsymbol{\tau}} \right] - \boldsymbol{e_z}$
- $Wi \overset{\nabla}{\tilde{\boldsymbol{\tau}}} + \max \left(0, \left(\frac{Ar}{1-\beta} \right)^{1-n} \frac{(\widetilde{\tau_d} - Bn)}{\widetilde{\tau_d}^{\,n}} \right)^{\frac{1}{n}} \tilde{\tau} = \frac{1-\beta}{Ar} \left(\widetilde{\boldsymbol{\nabla u}} + \widetilde{\boldsymbol{\nabla u}^T} \right)$
- $\frac{\rho}{\rho_1} = \tilde{\rho}(\phi) = \phi + \rho^{\circ}(1-\phi)$
- $\eta_1 = \eta_{s1} + k \left(\sqrt{\frac{g}{R}} \right)^{n-1}$

- ***Archimedes*** → *Buoyancy / Viscosity*
- ***Bond*** → *Buoyancy / Capillarity*
- ***Bingham*** → *Plasticity / Buoyancy*
- ***Weissenberg*** → *Elasticity / Viscosity*
- $\boldsymbol{\beta}$ → *Newtonian solvent contribution*

$$Ar = \frac{\rho_1 \sqrt{g R^3}}{\eta_1} \qquad Bo = \frac{\rho_1 g R^2}{\sigma} \qquad Bn = \frac{\tau_y}{\rho_1 g R} \qquad Wi = \frac{k}{G} \left(\sqrt{\frac{g}{R}} \right)^n \qquad \beta = \frac{\eta_{s1}}{\eta_{s1} + k \left(\sqrt{\frac{g}{R}} \right)^{n-1}}$$

Rheology

- 0.1 % Carbopol solution [*Lopez, Naccache, de Souza Mendez (LNM, JoR, 2018)]*.
- Parameters (k, n, τ_y) obtained through non-linear fitting of the flow curve.
- Elastic modulus (G) is obtained from SAOS experiments in linear viscoelastic regime.

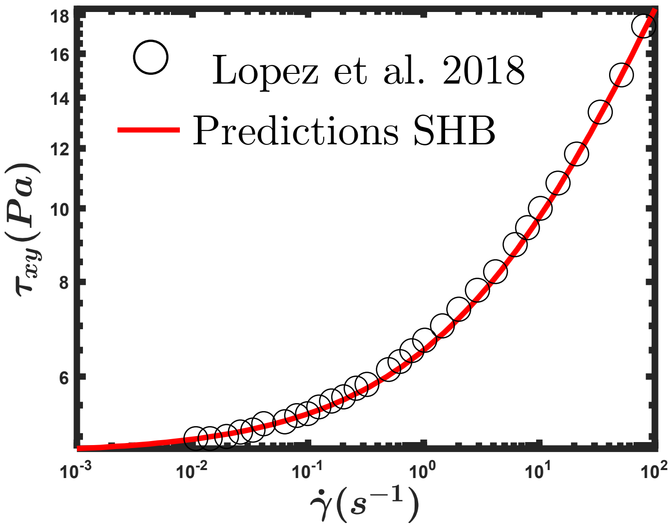

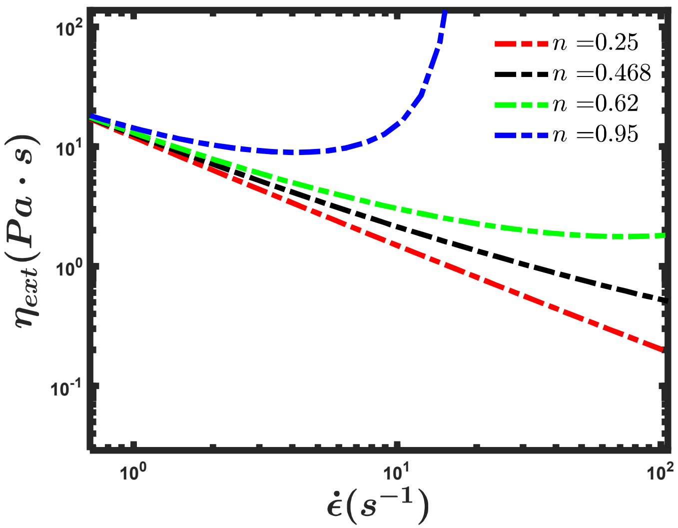

$$k = 1.75\ Pa \cdot s^n$$
$$\tau_y = 4.68\ Pa$$
$$n = 0.468$$
$$G = 40.42\ Pa$$
$$\beta = 0.01$$

Monotonic extension rate thinning for $n < 0.5$

Adaptive mesh refinement

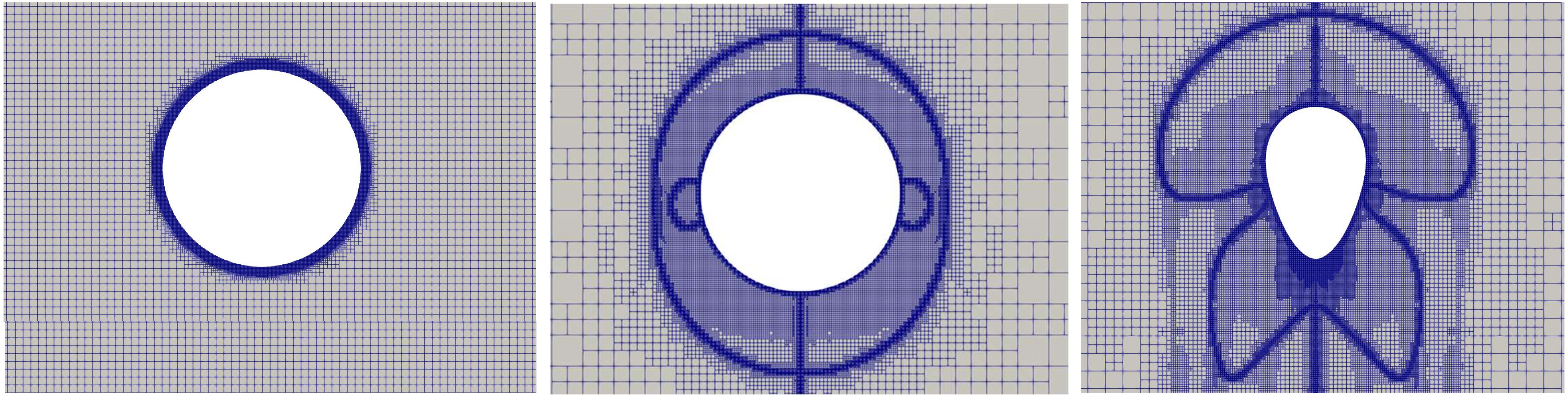

- **Initial refinement** around the bubble.
- Refinement is based on $\boldsymbol{\phi}, \boldsymbol{\tau}, \tilde{\boldsymbol{u}}, |\boldsymbol{\tau}_d - \boldsymbol{\tau}_y|$.
- **Max. Refinement** = 210 cells per bubble diameter.

- Max. Courant number = 0.1 → $\Delta t_{max} = O(10^{-3})$

R = 4.00 mm: terminal shape

- $Ar = 3.6$
- $Bo = 2.15$
- $Bn = 0.11$
- $Wi = 0.27$
- $\eta^{\circ} = 0.001$
- $\rho^{\circ} = 0.001$

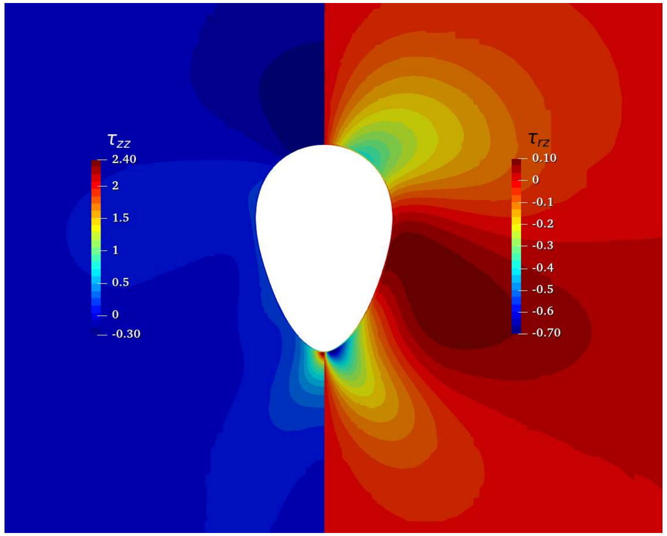

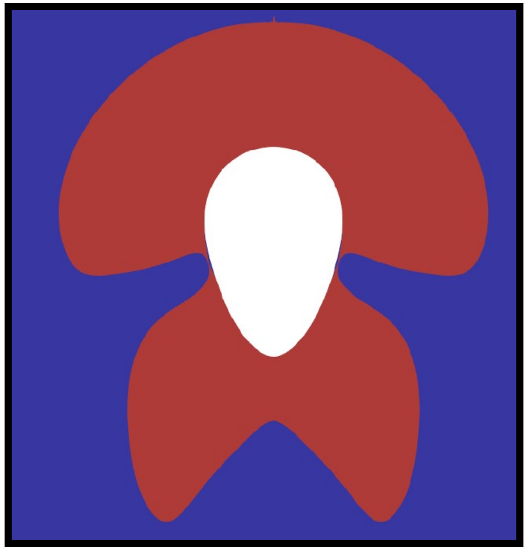

Yielded

Unyielded

Lopez, R = 4 mm

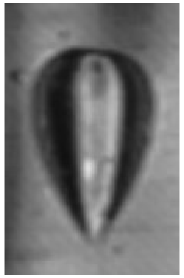

Carbopol, Dubash and Frigaard, JNNFM 2007

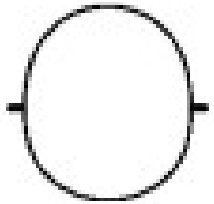

Tsamopoulos et al., JFM, 2008. BINGHAM model

- High axial extensional stresses at the rear of the bubble pull the interface downward.

- The characteristic **inverted teardrop shape** is observed in both experiments and simulations when elasticity is included.

R = 4.00 mm: transient evolution

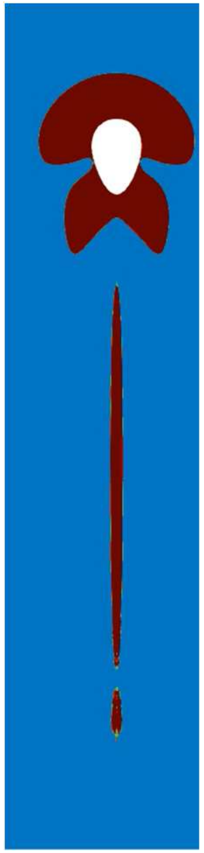

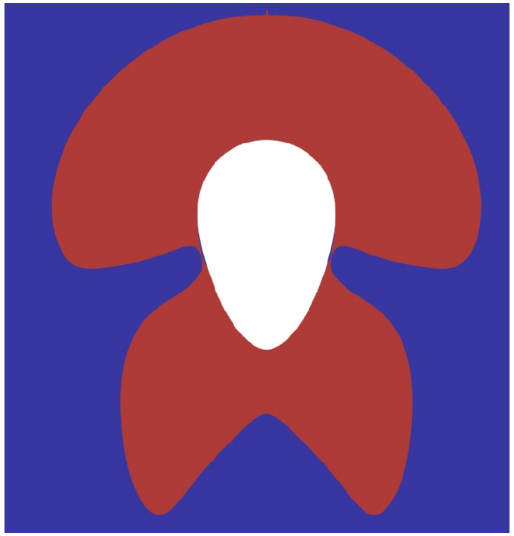

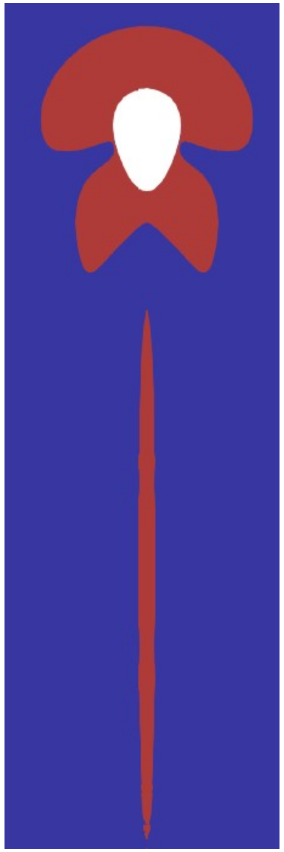

- The transient development of the prolate-shape makes the bubble decelerating.

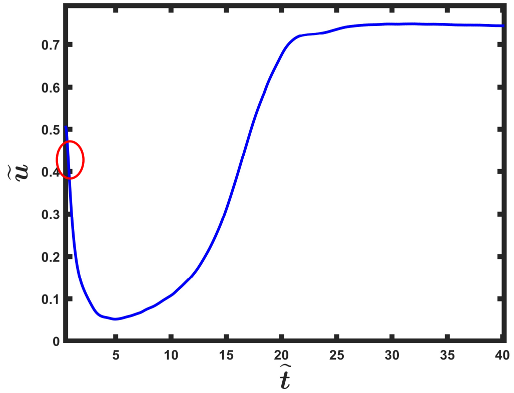

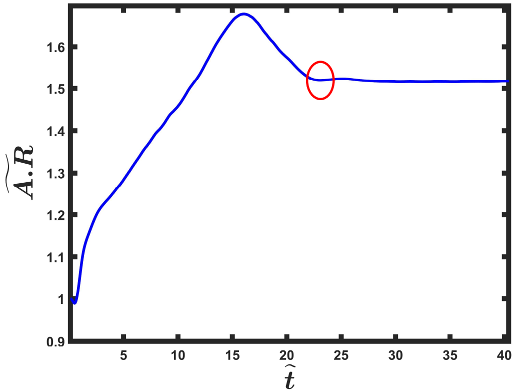

- First overshoot due to interplay between plasticity and buoyancy.

- Once the inverted teardrop shape is acquired, the higher terminal velocity is approached.

R = 4.00 mm: kinematic conditions

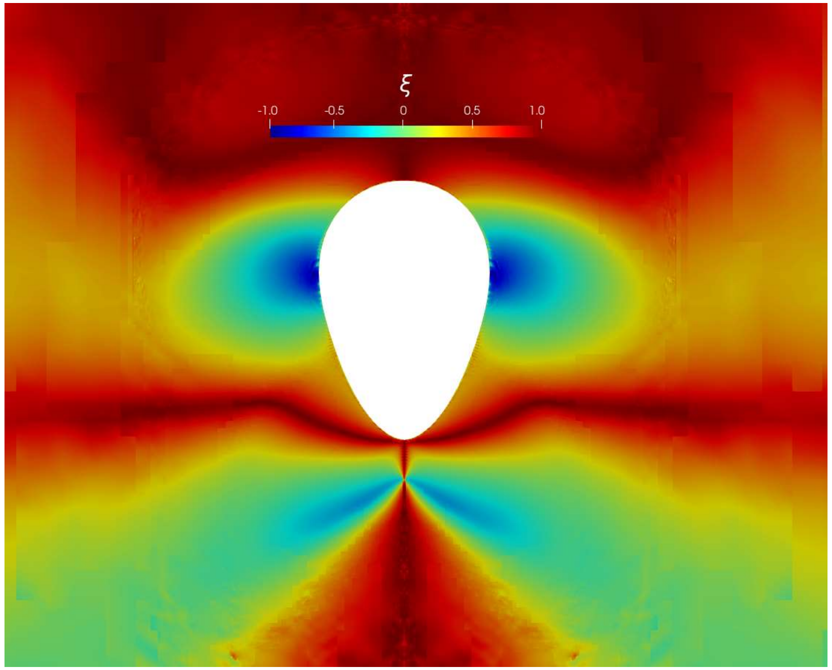

$$\xi = \frac{|\bar{D}| - |\bar{\Omega}|}{|\bar{D}| + |\bar{\Omega}|} \rightarrow \begin{cases} -1 & \text{Solid body rotation} \\ 0 & \text{Shear flow} \\ 1 & \text{Extensional flow} \end{cases}$$

$$\bar{D} = \frac{\nabla \mathbf{u} + \nabla \mathbf{u}^T}{2} \quad \bar{\Omega} = \frac{\nabla \mathbf{u} - \nabla \mathbf{u}^T}{2}$$

- $Ar = 20$
- $Bo = 34$
- $Bn = 0.03$
- $Wi = 0.19$
- $\eta^{\circ} = 0.001$
- $\rho^{\circ} = 0.001$

R = 16 mm → dominant inertia

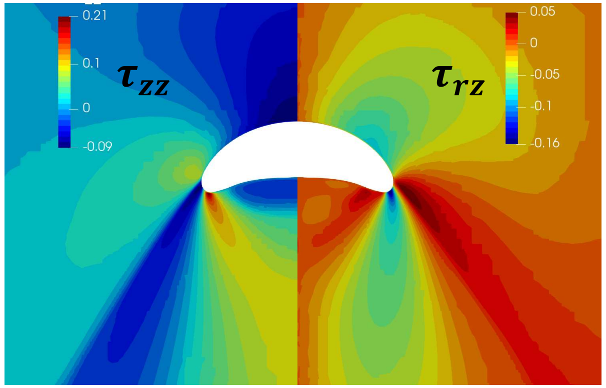

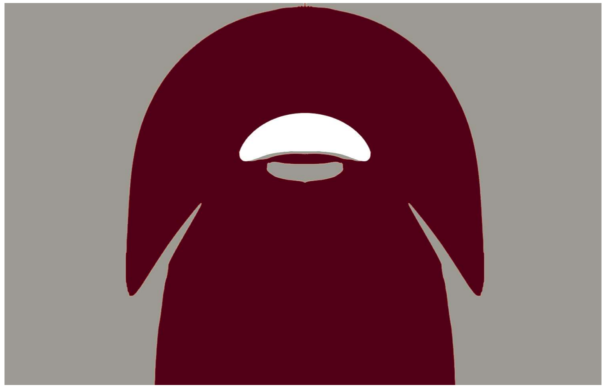

LNM, R = 16.2 mm.

- The **oblate** shape is a consequence of the dominant inertial effects
- The region at small rate of strain behind the indentation of the bubble resembles the results obtained in **Bingham** materials → **elasticity is subdominant.**

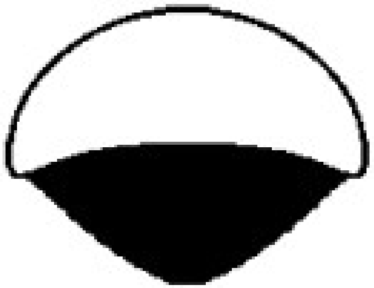

→ *Tsamopoulos, Dimakopoulos, Chatzidai, Karapetsas, Pavlidis, JFM, 2008.*

Bingham-Papanastasiou(no elasticity).

R = 8.30 mm → discrepancy

- $Ar = 8.93$
- $Bo = 9.26$
- $Bn = 0.057$
- $Wi = 0.225$
- $\eta^{\circ} = 0.001$
- $\rho^{\circ} = 0.001$

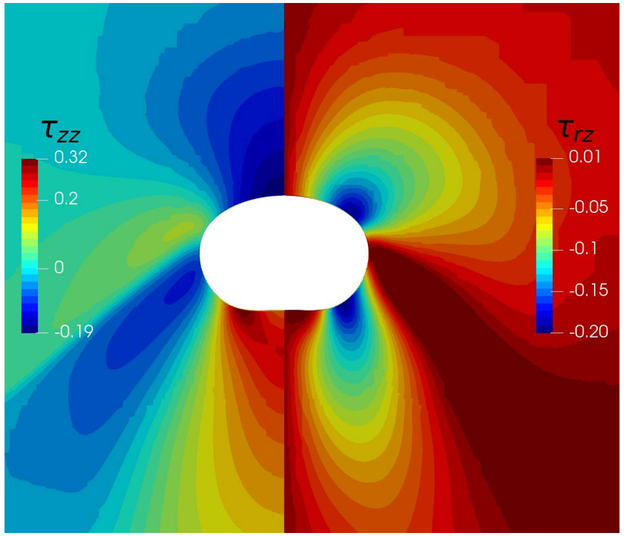

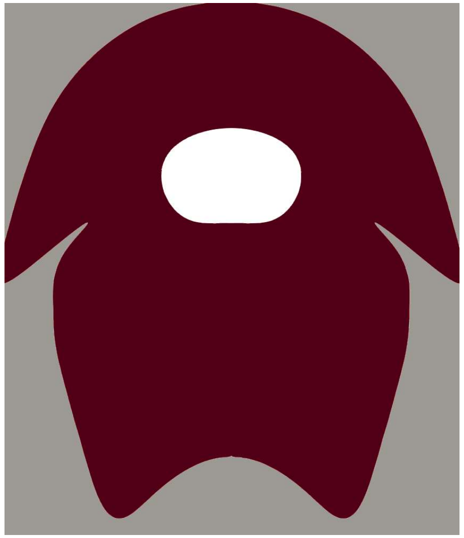

ξ

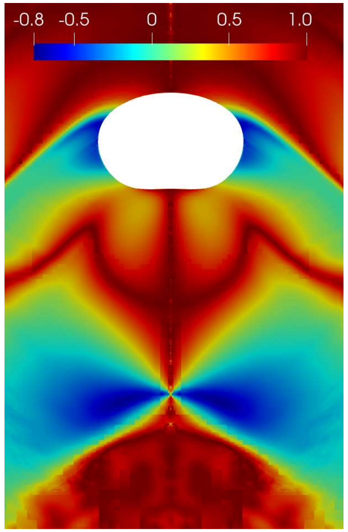

LNM, R = 8.3 mm

- Our numerical simulations predict an ***oblate*** shape indicating dominant inertia over elasticity
- The experimental results report an ***inverted teardrop shape*** → We underestimate the elastic response

R = 8.30 mm → discrepancy

$$Ar = \frac{\rho_1\sqrt{gR^3}}{\eta_1}$$

- The highest uncertainty is related to the **consistency** index *k*.
- Higher *k* causes higher Weissenberg (**elasticity**) and lower Archimedes (inertia)

$$Wi = \frac{k}{G}\left(\sqrt{\frac{g}{R}}\right)^n$$

$k = 1.81\ Pa \cdot s^n$ | $k = 2.5\ Pa \cdot s^n$ | $k = 3.4\ Pa \cdot s^n$ | $k = 5.3\ Pa \cdot s^n$

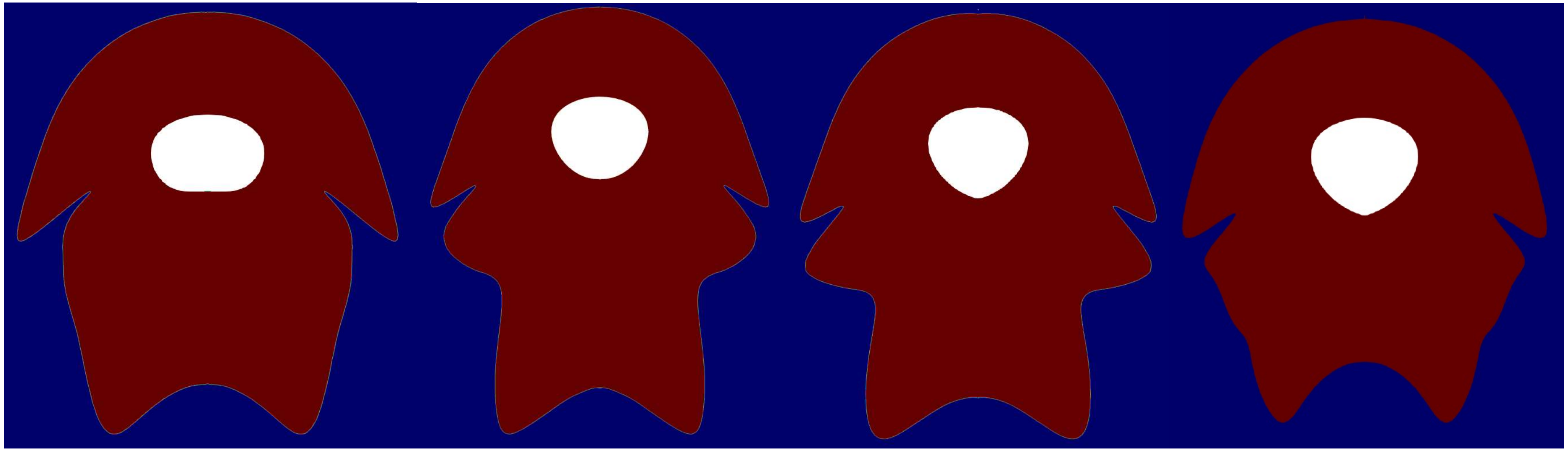

Negative wake and elasticity

- The **magnitude** of the negative wake increases with the elasticity of the fluid.
- The less elastic is the fluid, the **further** is located the negative wake and the more extended the region at negative velocity is.

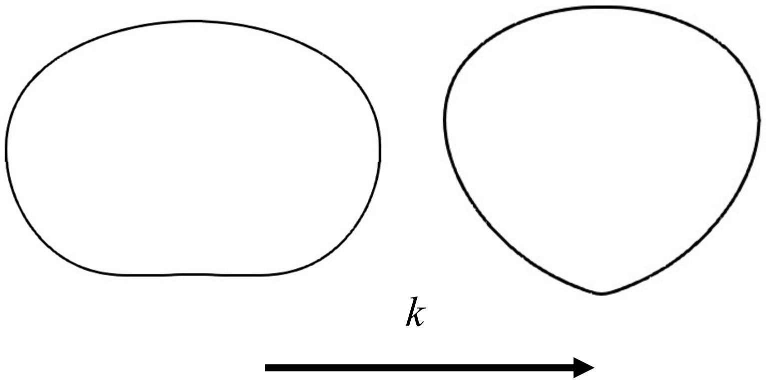

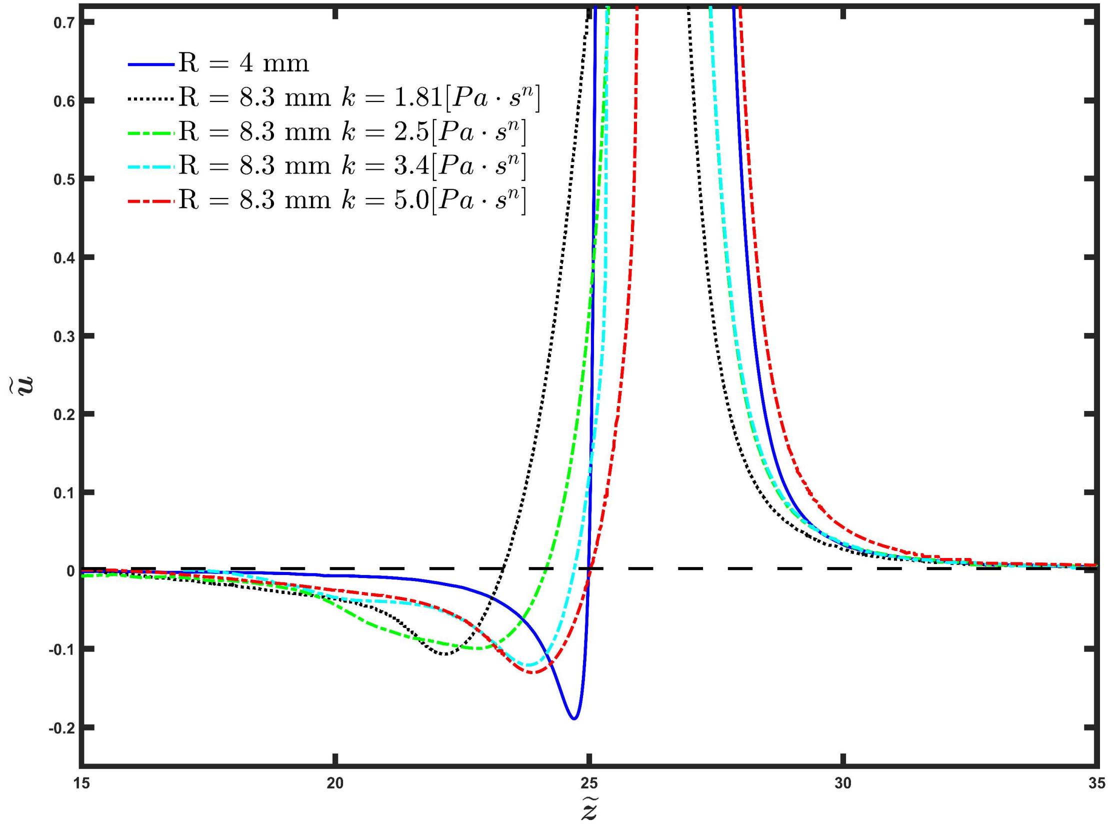

Comparison with experiments

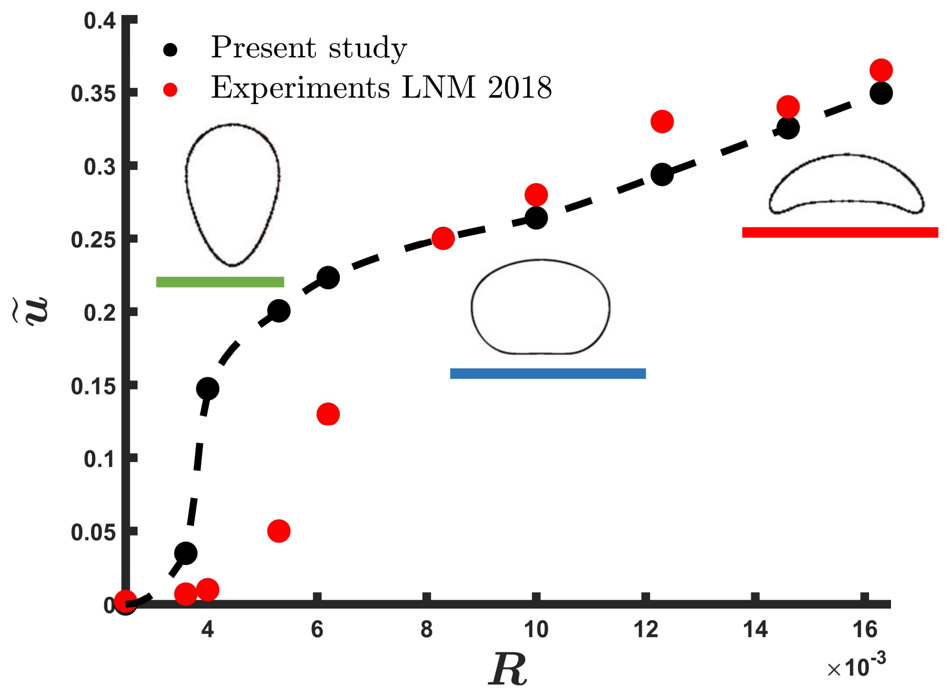

- Overprediction of the terminal velocity in the **elastic** regime.
- Quantitative agreement in terms of shapes and velocities in the **inertial** regime
- Quantitative agreement in terms of velocities for the **intermediate** regime, but a better rheological characterization is required.

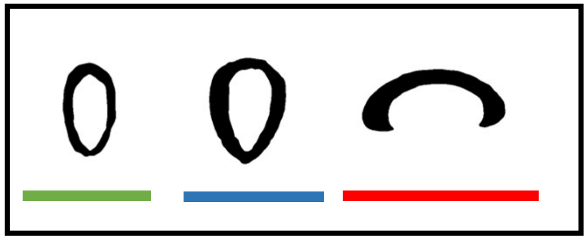

→ Experiments

Viscous drops in EVP materials

- $Ar = 16$
- $Bo = 20$
- $Bn = 0.01$
- $Wi = 0.42$
- $\eta^{\circ} = 0.005$
- $\rho^{\circ} = 0.765$

❑ Wobbling motion

❑ In Newtonian fluids, such oscillations are reported for high Reynolds.

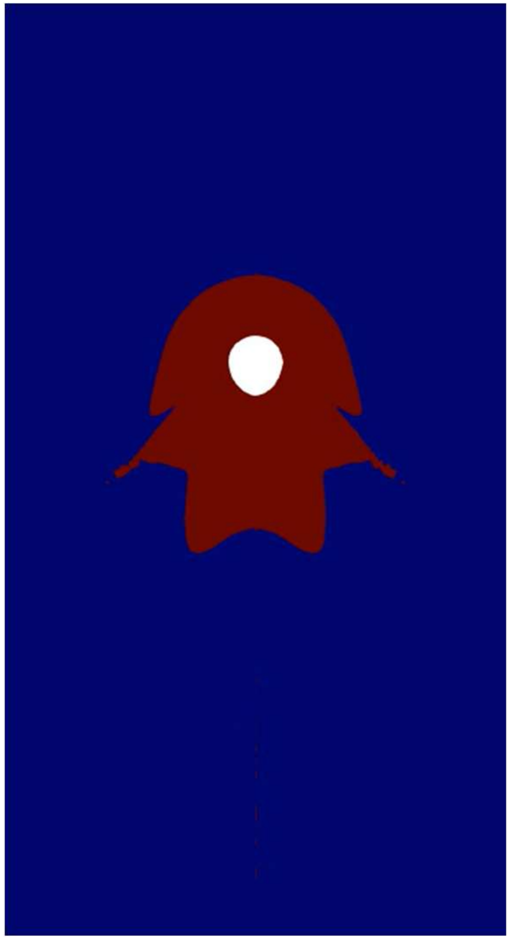

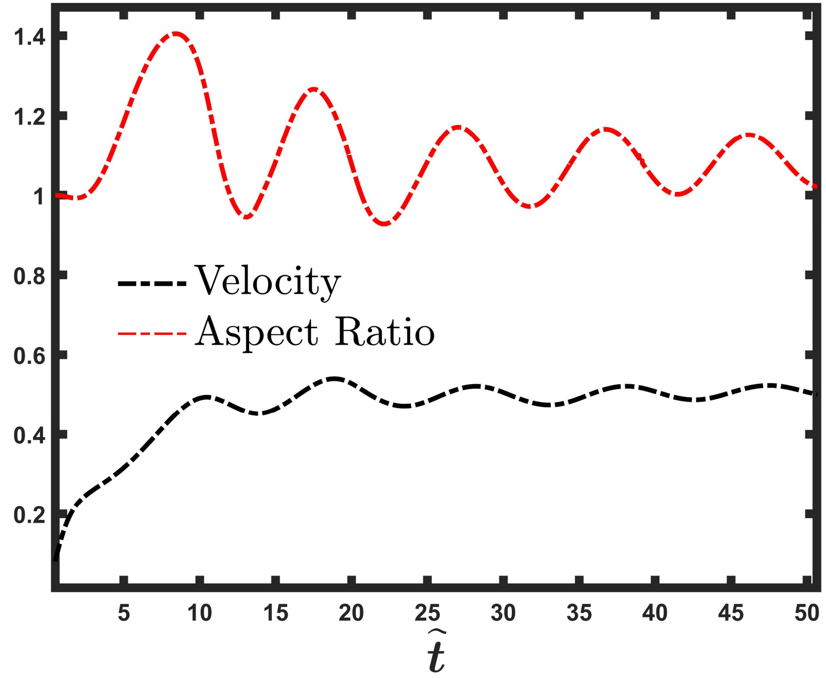

Drop of Toluene in LNM 0.1 %, R = 1 cm.

Viscous drops in EVP materials

- The yield surface around a viscous drop sedimenting into a EVP fluid **resembles qualitatively** the one observed for smooth spheres.
- A comparison with the magnitude of the velocity field, highlights a **discrepancy** between the predictions in terms of stresses (Von Mises criterion) and velocities (solid regions where the velocity is small)

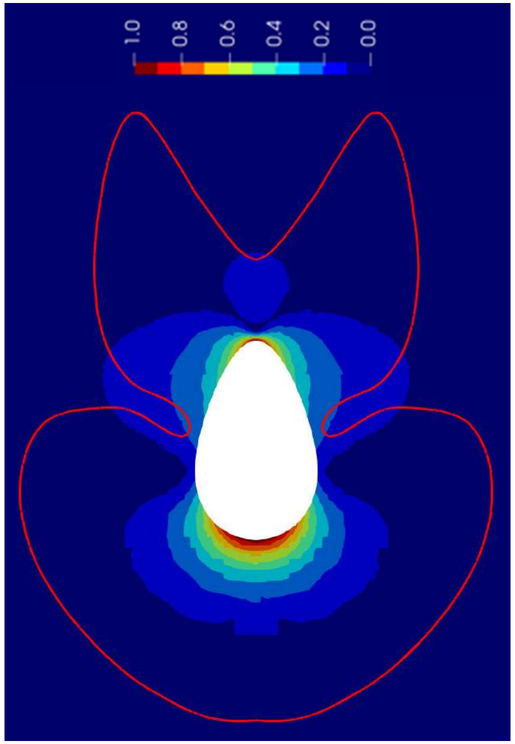

Present study (DROP)

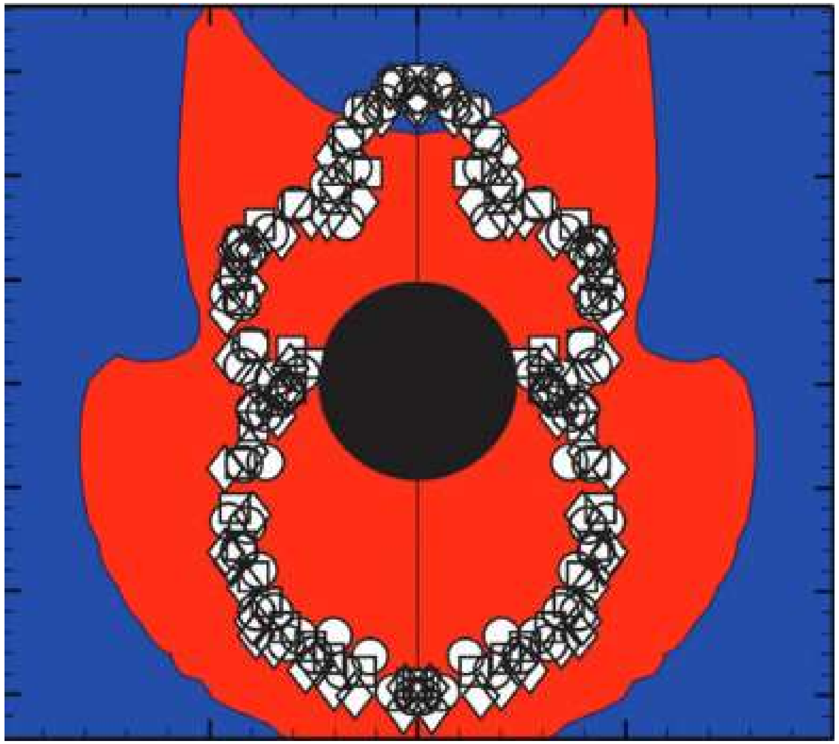

Fraggedakis, Dimakopoulos, Tsamopoulos, 2016, Soft Matter.

- $Ar = 9.68$
- $Bo = 9.65$
- $Bn = 0.015$
- $Wi = 0.45$
- $\eta^{\circ} = 0.1, \rho^{\circ} = 1.265$

What if we consider more than 2 materials?

- The recent experiment of Pourzahedi, Zare & Frigaard, 2021, JNNFM, shows that the inverted teardrop shape is caused by the elasticity of the material rather than injection conditions.
- We can numerically reproduce a similar setup: bubble rising in two fluids (Newtonian-EVP) or three fluids (EVP-Newtonian-EVP).
- In Basilisk, we use **three-phase.h** and **tension_three-phase.h**

N – E - B

Bubble rising in multilayer systems

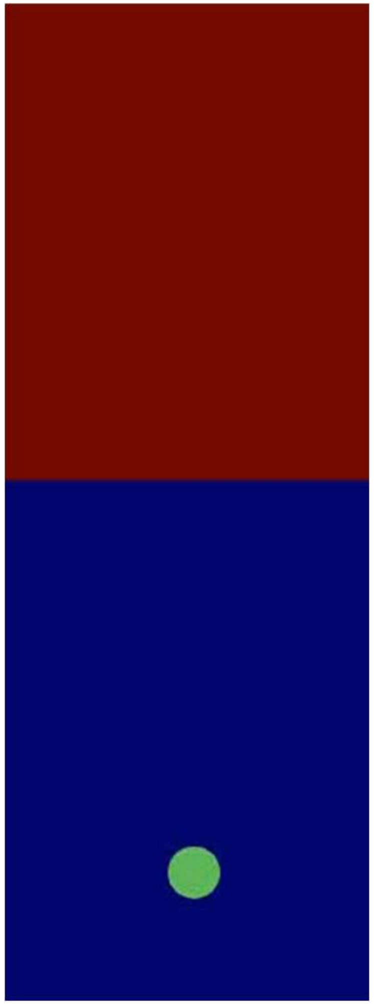

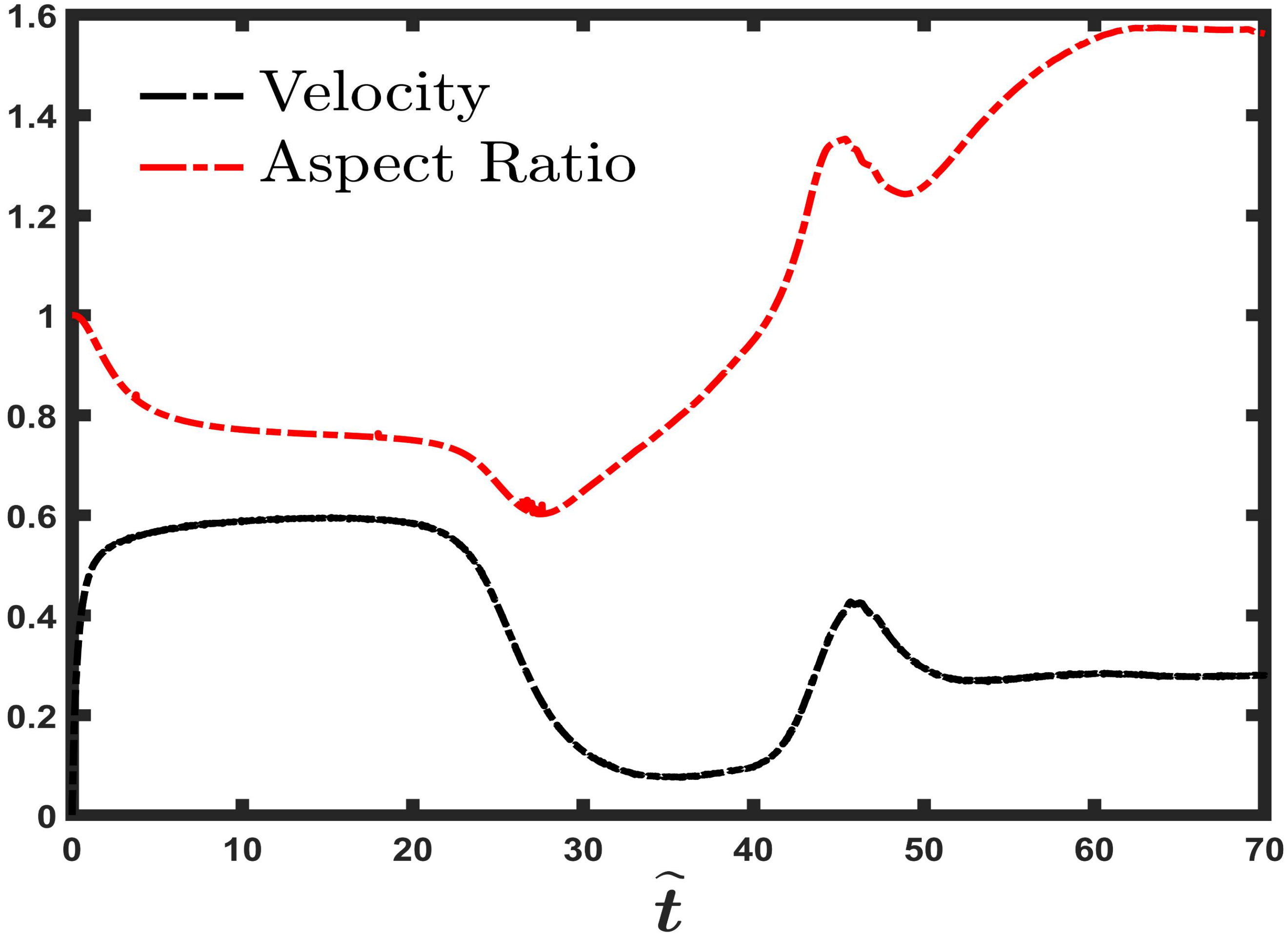

Future work

- Complete study of a single viscous drop sedimenting in EVP materials.
- **Hydrodynamic interactions** of two co-axial bubbles and drops (equal and unequal size) under the assumption of axial symmetry.
- Bubble / drop rising in stratified complex fluids (EVP, Viscoelastic).
- 3D Formulation for complex fluids?

THANK YOU!

Ευχαριστώ πολύ
Merci Beaucoup
Grazie mille
Grazie assaje!